Pcsk9 Deletion Promotes Murine Nonalcoholic Steatohepatitis and Hepatic Carcinogenesis: Role of Cholesterol

George N. Ioannou ,[1-3] Sum P. Lee,[2] Peter S. Linsley,[4] Vivian Gersuk,[4] Matthew M. Yeh,[2,5] Yen-Ying Chen,[5,6,*] Yi-Jen Peng,[5,7] Moumita Dutta,[8] Gabby Mascarinas,[8] Bruk Molla,[8] Julia Yue Cui,[8] and Christopher Savard[1-3]

Proprotein convertase subtilisin/kexin type 9 (Pcsk9) binds to hepatic low-density lipoprotein receptor (LDLR) and induces its internalization and degradation. Pcsk9 inhibition increases LDLR expression by hepatocytes, which causes increased uptake of circulating LDL, thereby reducing plasma LDL-cholesterol. However, by increasing the uptake of LDL by the liver, Pcsk9 inhibition increases the exposure of the liver to cholesterol, which may result in higher risk of steatohepatitis and ever carcinogenesis. We compared *Pcsk9*-/- knockout (KO) mice and appropriate wild-type (WT) controls of the same strain assigned to a high-fat (15%, wt/wt) diet for 9 months supplemented with 0.25%, 0.5%, or 0.75% dietary cholesterol. *Pcsk9* KO mice on a high-fat, high-cholesterol diet exhibited higher levels of hepatic free cholesterol loading and hepatic cholesterol crystallization than their WT counterparts. *Pcsk9* KO mice developed crown-like structures of macrophages surrounding cholesterol crystal-containing lipid droplets and hepatocytes, exhibited higher levels of apoptosis, and developed significantly more hepatic inflammation and fibrosis consistent with fibrosing steatohepatitis, including 5-fold and 11-fold more fibrosis at 0.5% and 0.75% dietary cholesterol, respectively. When injected with diethylnitrosamine, a hepatic carcinogen, early-in-life *Pcsk9* KO mice were more likely to develop liver cancer than WT mice. *Conclusion: Pcsk9* KO mice on high-cholesterol diets developed increased hepatic free cholesterol and cholesterol crystals and fibrosing steatohepatitis with a higher predisposition to liver cancer compared with WT mice. Future studies should evaluate whether patients on long-term treatment with anti-PSCK9 monoclonal antibodies are at increased risk of hepatic steatosis, steatohepatitis or liver cancer, while accounting for concurrent use of statins. (*Hepatology Communications* 2022;6:780-794).

Proprotein convertase subtilisin/kexin type 9 (PCSK9) is a circulating protein secreted primarily by the liver; it binds to hepatic low-density lipoprotein receptor (LDLR) and induces its internalization and degradation. Thus, PCSK9 reduces the expression of LDLR by hepatocytes and increases plasma LDL-cholesterol. Conversely, inhibition of PCSK9 increases LDLR expression by hepatocytes, which causes increased uptake of circulating LDL, thereby reducing plasma LDL-cholesterol. Accordingly, *Pcsk9* knockout mice have hypocholesterolemia, with high levels of hepatic LDLR protein and lower levels of LDL-cholesterol.[1] In humans, gain-of-function mutations in PCSK9 lead to extremely

Abbreviations: AST, aspartate aminotransferase; ALT, alanine aminotransferase; ER, endoplasmic reticulum; HMW, high molecular weight; HOMA-IR, Homeostasis Model Assessment–Insulin Resistance; LDLR, low-density lipoprotein receptor; NAFLD, nonalcoholic fatty liver disease; NASH, nonalcoholic steatohepatitis; Pcsk9, proprotein convertase subtilisin/kexin type 9; TUNEL, terminal deoxynucleotidyl transferase–mediated deoxyuridine triphosphate nick-end labeling.

Received May 28, 2021; accepted October 14, 2021.

Additional Supporting Information may be found at onlinelibrary.wiley.com/doi/10.1002/hep4.1858/suppinfo.

Supported by the National Institute of Diabetes and Digestive and Kidney Diseases (DK017047) and U.S. Department of Veterans Affairs (BX002910).

Role of Funding Source: The funding source played no role in study design, collection, analysis or interpretation of data.

Disclaimer: The contents do not represent the views of the U.S. Department of Veterans Affairs or the United States Government.

**Department of Pathology, Shuang Ho Hospital and School of Medicine, College of Medicine, Taipei Medical University, Taipei, Taiwan*

high plasma cholesterol levels of >500 mg/dL, while loss-of-function mutations lead to very low LDL-cholesterol levels and dramatic reductions in lifetime risk of cardiovascular disease.[2-4] Neutralizing antibodies that inhibit PCSK9 binding to LDLR have been approved in Europe and the United States since 2015 (alirocumab by Regeneron/Sanofi in 2015 and evolocumab by Amgen in 2017) as second-line treatments for hypercholesterolemia not controlled by diet and statin therapy.[5]

Nonalcoholic fatty liver disease (NAFLD) is the most common liver disease in the world, and is associated with obesity, diabetes, metabolic syndrome, insulin resistance and hyperlipidemia. The impact of long-term PCSK9 inhibition on NAFLD is unclear. In general, factors that are associated with hyperlipidemia and hypercholesterolemia tend to be associated with fatty liver disease and vice versa. Statins, which inhibit cholesterol synthesis in the liver and reduce plasma LDL-cholesterol, appear to be associated with a reduction in the risk of NAFLD and nonalcoholic steatohepatitis (NASH).[6-11] By that analogy, PCSK9 inhibitors, which also reduce plasma LDL-cholesterol, might be expected to reduce hepatic steatosis too. In fact, it has been postulated that PCSK9 inhibitors might ameliorate NAFLD, independently of their known beneficial effects on reduction of LDL-cholesterol and cardiovascular disease.[12]

However, PCSK9 inhibitors reduce plasma LDL-cholesterol by directly increasing the expression of LDLRs on hepatocytes, thereby increasing LDL-cholesterol uptake by hepatocytes. Thus, PCSK9 inhibition might be expected to result in greater exposure of the liver to cholesterol. In contrast, statins increase the expression of LDLRs by inhibiting the synthesis of cholesterol in hepatocytes, thereby resulting in lower exposure of the liver to excess cholesterol. Therefore, although both statins and PCSK9 inhibitors reduce plasma LDL-cholesterol and reduce cardiovascular outcomes, statins decrease hepatic cholesterol exposure, whereas PCSK9 inhibitors may increase hepatic cholesterol exposure.

Several lines of evidence suggest that hepatic free cholesterol is an important etiologic factor that can lead to the development and progression from simple steatosis to fibrosing steatohepatitis and hepatocarcinogenesis, both in animal models and in humans.[13] We also demonstrated in both humans and mice that excess cholesterol crystallizes in hepatocyte lipid droplets, and these cholesterol crystals might promote necroinflammation in NASH.[14-17] In this study, we aimed to determine whether *Pcsk9* deletion leads to hepatic cholesterol loading and crystallization in the setting of a high-fat, high-cholesterol diet in mice, promoting the development of fibrosing steatohepatitis and liver cancer.

View this article online at wileyonlinelibrary.com.
DOI 10.1002/hep4.1858

Potential conflict of interest: Nothing to report.

ARTICLE INFORMATION:

From the [1]Division of Gastroenterology, Department of Medicine, Veterans Affairs Puget Sound Health Care System, Seattle, WA, USA; [2]Division of Gastroenterology, Department of Medicine, University of Washington, Seattle, WA, USA; [3]Research and Development, Veterans Affairs Puget Sound Health Care System, Seattle, WA, USA; [4]Systems Immunology, Benaroya Research Institute, Seattle, WA, USA; [5]Department of Laboratory Medicine and Pathology, University of Washington, Seattle, WA, USA; [6]Department of Pathology and Laboratory Medicine, School of Medicine, Taipei Veterans General Hospital, National Yang-Ming University, Taipei, Taiwan; [7]Department of Pathology, Tri-Service General Hospital, National Defense Medical Center, Taipei, Taiwan; [8]Department of Environmental and Occupational Health Sciences, University of Washington, Seattle, WA, USA.

ADDRESS CORRESPONDENCE AND REPRINT REQUESTS TO:

George Ioannou, B.M.B.Ch., M.S.
Veterans Affairs Puget Sound Health Care System,
Gastroenterology
S-111-Gastro
1660 S. Columbian Way
Seattle, WA 98108, USA
E-mail: georgei@medicine.washington.edu
Tel.: +1-206-277-3136

Methods

ANIMAL PROCEDURES

B6;129S6-Pcsk9^{tm1Jdh}/J mice, with homozygous *Pcsk9*-/- knockout (KO) mutations and appropriate wild-type (WT) controls of the same strain (B6;129S F1/J) were purchased from the Jackson Laboratory (Bar Harbor, ME). The *Pcsk9* KO mice were not littermates of the WT mice. WT and *Pcsk9* KO mice were assigned to a high-fat (15%, wt/wt) diet for 9 months supplemented with 0.25%, 0.5%, or 0.75% dietary cholesterol (six groups, n = 12 mice/group). Cocoa butter, which contains approximately 60% saturated fat, was the source of the extra fat in these diets.[14,16] Their composition is given in Supporting Table S1.

An additional group of WT (n = 6) and Pcsk9 KO (n = 6) assigned to a high-fat (15%) diet with 0.75% cholesterol for 9 months were injected intraperitoneally at 5 weeks of age with 50 mg/kg body weight of diethylnitrosamine (DEN), which can induce hepatic carcinogenesis.[18,19] Separate groups of mice injected a higher dose (100 mg/kg) of DEN exhibited signs of distress and had to be euthanized.

Mice were housed up to four per cage with unrestricted access to food and water. Mice underwent phlebotomy and were euthanized 9 months after initiation of the experimental diets by cervical dislocation following isoflurane anesthesia, and their livers were harvested for studies as outlined subsequently. All experimental procedures were approved by the Institutional Animal Care and Use Committee of the Veterans Affairs Puget Sound Health Care System.

HISTOLOGICAL ASSESSMENT OF STEATOSIS, INFLAMMATION, FIBROSIS, APOPTOSIS, AND CARCINOGENESIS

Formalin-fixed, paraffin-embedded liver tissue sections were stained with hematoxylin and eosin, Masson's trichrome, or sirius red (for collagen). Histological steatosis, inflammation, and fibrosis were assessed semi-quantitatively using the scoring system of Kleiner et al.[20] in a "blinded" fashion at consensus by pathologists with experience in liver pathology (Y.Y.C., Y.J.P., and M.M.Y.). Sirius red–stained collagen fibers were also quantified using a polarizing microscope by digital image analysis (NIH Image J density software), as the average of 12 random ×200 fields without major blood vessels.[21] Anti-CD68 antibody was used to stain for macrophages and quantified by digital image analysis of 12 random ×200 fields. Apoptotic cells were identified using a terminal deoxynucleotidyl transferase–mediated deoxyuridine triphosphate nick-end labeling (TUNEL) immunohistochemistry detection kit and the number of TUNEL-positive cells counted and averaged in 12 random ×100 fields.

Harvested, whole livers were inspected macroscopically for visible masses, which were excised, sectioned, and stained as previously to confirm whether they had histological features of hepatocellular carcinoma. Additionally, each liver lobe was sliced into parallel sections approximately 2-3 mm apart to evaluate macroscopically and microscopically for hepatocellular carcinoma.

ASSESSMENT OF HEPATOCYTE CHOLESTEROL CRYSTALS, FREE CHOLESTEROL STAINING, AND LIPID DROPLETS

Fresh-frozen liver tissue was embedded in Optimal Cutting Temperature compound and sectioned at 10 μm in thickness. Sections were allowed to come to room temperature, immediately cover-slipped using pure glycerol as the mounting medium without applying any stain and examined using a Nikon Eclipse microscope with and without a polarizing filter, to evaluate for the presence of birefringent crystals typical of cholesterol crystals.[4,5,18] Cholesterol crystals were quantified using a polarizing microscope for digital image analysis as mentioned previously. Osmium was used to stain and fix lipid droplets.

Frozen liver sections were stained with filipin, which identifies free cholesterol by interacting with its 3β-hydroxy group to fluoresce blue,[14,22] and examined using a Nikon Eclipse fluorescence microscope with an excitation 340-380/ emission 435-485 filter in place.

HEPATIC LIPID ANALYSIS

Lipids were extracted using dichloromethane/methanol after the addition of 54 isotope labeled internal standards. The extracts were concentrated under nitrogen and reconstituted in 10 mM ammonium

acetate in dichloromethane:methanol (50:50). Lipids were analyzed using the Sciex Lipidyzer platform consisting of a Shimadzu LC and AB Sciex QTRAP 5500 MS/MS system equipped with SelexION for differential mobility spectrometry (DMS). Multiple reaction monitoring was used to target and quantify lipids in positive and negative ionization modes with and without DMS.

Free cholesterol was extracted with water, methanol, and chloroform solvents (1:1:1 vol/vol/vol). The chloroform fractions were dried using nitrogen gas and the residues were dissolved in deuterated chloroform. Nuclear magnetic resonance spectra were obtained using a 800-MHz Bruker Avance III spectrometer. Free cholesterol signal was identified, and its concentration was obtained using the residual solvent signal from the solvent as the internal reference.

Liquid chromatographic separation and mass spectrometric detection for bile acids were performed using the Agilent G6460 UPLC-MS/MS system combined with a triple quadropole mass spectrometer with an electrospray ionization interface.[23]

HEPATIC GENE-EXPRESSION STUDIES BY RNA SEQUENCING

Total RNA was isolated from frozen mouse liver. RNA (0.5 ng) was reverse-transcribed into full-length amplified complementary DNA. Dual-index, single-read sequencing of pooled libraries was carried out on a HiSeq2500 sequencer (Illumina) with a target depth of 5 million reads per sample. Basecalls were processed to FASTQs on BaseSpace (Illumina), and a base call quality trimming step was applied to remove low-confidence base calls from the ends of reads. The FASTQs were aligned to the mouse reference genome using STAR v.2.4.2a, and gene counts were generated using htseq-count. QC and metrics analysis was performed using the Picard family of tools (v1.134).[24]

OTHER MEASUREMENTS

Blood specimens were collected immediately before sacrifice after a 4-hour fast and tested for plasma cholesterol, triglycerides, alanine aminotransferase (ALT), aspartate aminotransferase (AST), alkaline phosphatase, glucose, insulin, and high molecular weight (HMW) adiponectin. Average food consumption was measured monthly.

Results

PCSK9 KO MICE ACCUMULATED MORE HEPATIC FREE CHOLESTEROL AND CHOLESTEROL CRYSTALS THAN WT MICE WHEN FED HIGH-CHOLESTEROL DIETS

Filipin staining of free cholesterol increased progressively with increasing dietary cholesterol concentration (0.25%, 0.50%, and 0.75%), and was significantly higher in the *Pcsk9* KO mice than the WT mice at 0.50% or 0.75% dietary cholesterol (Table 1 and Fig. 1). This was mirrored in the presence of hepatic cholesterol crystals, which were more prominent in the *Pcsk9* than the WT mice at 0.50% and 0.75% dietary cholesterol (Table 1 and Fig. 1). At 0.75% dietary cholesterol, prominent filipin staining was observed in the periphery of lipid droplets in *Pcsk9* KO mice in association with cholesterol crystals (Fig. 2).

Hepatic lipid analyses in mice fed a 0.75% cholesterol diet demonstrated that free cholesterol was the only major lipid class that was significantly increased in *Pcsk9* KO versus WT mice both in composition (i.e., as a percentage of all lipids) and in concentration (i.e., per gram of liver) (Table 2). In contrast, triglycerides, cholesterol esters, free fatty acids, and phospholipids were similar in *Pcsk9* KO and WT mice when expressed a composition and lower in *Pcsk9* KO than WT mice when expressed as concentration. The concentration of hepatic bile acids was similar in *Pcsk9* KO and WT mice (Table 2).

PCSK9 KO MICE DEVELOPED SIGNIFICANTLY HIGHER HEPATIC NECROINFLAMMATION AND FIBROSIS THAN WT MICE WHEN FED HIGH-CHOLESTEROL DIETS, ASSOCIATED WITH MACROPHAGE CROWN-LIKE STRUCTURES

At higher concentrations of dietary cholesterol (0.5% and 0.75%), the *Pcsk9* KO mice developed significantly higher hepatic necroinflammation than their WT counterparts, as evidenced by significantly

TABLE 1. COMPARISON OF *PCSK9* KO AND WT MICE WITH RESPECT TO BODY AND LIVER WEIGHTS, HEPATIC LIPID COMPOSITION, PLASMA LEVELS AND HEPATIC HISTOLOGY, AFTER 9 MONTHS ON HIGH-FAT DIETS SUPPLEMENTED WITH DIFFERENT CONCENTRATIONS OF DIETARY CHOLESTEROL (MEAN ± SD)

Diet	0.25% Cholesterol (n = 12)	0.25% Cholesterol (n = 12)	0.5% Cholesterol (n = 12)	0.5% Cholesterol (n = 12)	0.75% Cholesterol (n = 12)	0.75% Cholesterol (n = 12)	0.75% Cholesterol + DEN (n = 6)	0.75% Cholesterol + DEN (n = 6)
Genetic background	WT	*Pcsk9* KO	WT	*Pcsk9* KO	WT	*Pcsk9* KO	WT	*Pcsk9* KO
Body weight (g)	47.9 ± 3.5	46.6 ± 7.0	49.5 ± 4.2	52.5 ± 2.9	54.2 ± 5.1	55.1 ± 5.4	51.7 ± 7.2	49.1 ± 5.1
Liver weight (g)	2.4 ± 0.7	2.7 ± 1.1	2.9 ± 1.0	4.4 ± 0.8*	3.9 ± 1.3	4.0 ± 0.8	3.0 ± 1.3	3.6 ± 0.5
Liver weight/body weight (%)	5.0 ± 1.2	5.7 ± 1.4	5.7 ± 1.5	8.4 ± 1.2*	6.9 ± 2.1	7.3 ± 1.3	5.5 ± 1.8	7.4 ± 1.8
Food consumption (g/mouse/day)	3.0 ± 0.1	3.2 ± 0.2	3.4 ± 0.2	3.4 ± 0.2	4.0 ± 0.1	3.5 ± 0.2	4.0 ± 0.1	4.0 ± 0.2
PLASMA LEVELS (fasting)								
ALT (U/L)	83.3 ± 82.6	146.8 ± 160.8	111.3 ± 162.9	279.6 ± 183.6*	123.5 ± 64.2	242.5 ± 79.2*	92.2 ± 72.9	264.7 ± 111.5*
AST (U/L)	96.3 ± 87.4	108.6 ± 109.9	98.8 ± 98.7	197.9 ± 105.3*	110.5 ± 45.2	179.3 ± 53.7*	100.0 ± 66.9	300.2 ± 281.6
ALP (U/L)	73.9 ± 29.6	97.8 ± 49.1	78.4 ± 46.9	156.4 ± 70.3*	92.2 ± 48.5	160.7 ± 34.5*	80.4 ± 20.5	144.3 ± 48.8*
Cholesterol (mg/dL)	226.6 ± 31.2	168.6 ± 40.0*	226.9 ± 29.0	232.9 ± 35.4	236.0 ± 50.6	206.8 ± 37.9*	169.6 ± 78.9	143.2 ± 42.7
Triglyceride (mg/dL)	74.0 ± 20.3[+]	93.8 ± 21.0[+]	74.7 ± 18.9	75.3 ± 21.8	77.2 ± 19.3	59.9 ± 10.3*	65.8 ± 14.1	62.5 ± 15.6
Glucose (mg/dL)	257.5 ± 37.4	285.0 ± 48.0	265.4 ± 41.4	332.2 ± 37.0*	242.7 ± 38.3	263.3 ± 34.1	N/A	N/A
Insulin (ng/mL)	3.25 ± 1.76	4.87 ± 2.46	4.19 ± 1.67	5.59 ± 2.81	2.22 ± 1.37	3.54 ± 2.11	N/A	N/A
HOMA-IR[§]	52.7 ± 25.2	93.2 ± 25.3*	67.4 ± 23.7	115.4 ± 58.8*	32.8 ± 20.1	60.5 ± 41.3*	N/A	N/A
HMW-Adiponectin (μg/mL)	3.29 ± 0.66	5.41 ± 1.33*	3.58 ± 2.07	3.69 ± 0.82	2.29 ± 0.81	4.69 ± 1.67*	N/A	N/A
HEPATIC HISTOLOGY								
Steatosis (0-3)[†]	3	3	2	3	3	3	3	3
Inflammation (0-3)[†]	1	1	1	2	2	3	1	2
Fibrosis (0-4)[†]	0	0	0	1	1	2	0	2
Sirius red staining (fibrosis)[‡], % area	0.06 ± 0.03	0.06 ± 0.03	0.03 ± 0.02	0.16 ± 0.12*	0.19 ± 0.21	2.09 ± 1.26*	0.04 ± 0.04	0.91 ± 1.0
Cholesterol crystals[‡], % area	0.07 ± 0.08	0.03 ± 0.05	0.22 ± 0.22	0.45 ± 0.62	1.03 ± 1.58	1.69 ± 1.31*	0.18 ± 0.21	0.75 ± 0.57

Lobular Inflammation combines foci of mononuclear, fat granulomas, and polymorphonuclear leucocytes and is graded at ×200 magnification: no foci, 0; one focus, 1; two to four foci, 2; >four foci, 3 (per ×200 field).
Fibrosis is staged as none, 0; perisinusoidal or periportal, 1; periportal and perisinusoidal, 2; bridging fibrosis, 3; and cirrhosis, 4.[20]
N/A, not applicable: Three of six DEN-injected mice had liver cancer at the time of sacrifice, resulting in spuriously abnormal levels.
*Statistically significant differences between the *Pcsk9* KO and WT mice are shown by asterisks (*) for $P < 0.05$, using the Student's t test.
[†]Median values are reported for histological steatosis, inflammation, and fibrosis scored as follows[20]: Steatosis is graded based on the proportion of hepatocytes being steatotic at ×200 magnification (<5%, 0); 5%-33%, 1; 34%-66%, 2; >66%, 3).
[‡]Presented as the percentage of the surface area of the liver section that is positive for sirius red or cholesterol crystals and calculated as the average of 10 random ×200 fields.
[§]HOMA-IR was calculated as HOMA-IR = (insulin [mmol/L] × (glucose [mmol/L])/22.5.
Abbreviation: ALP, alkaline phosphatase.

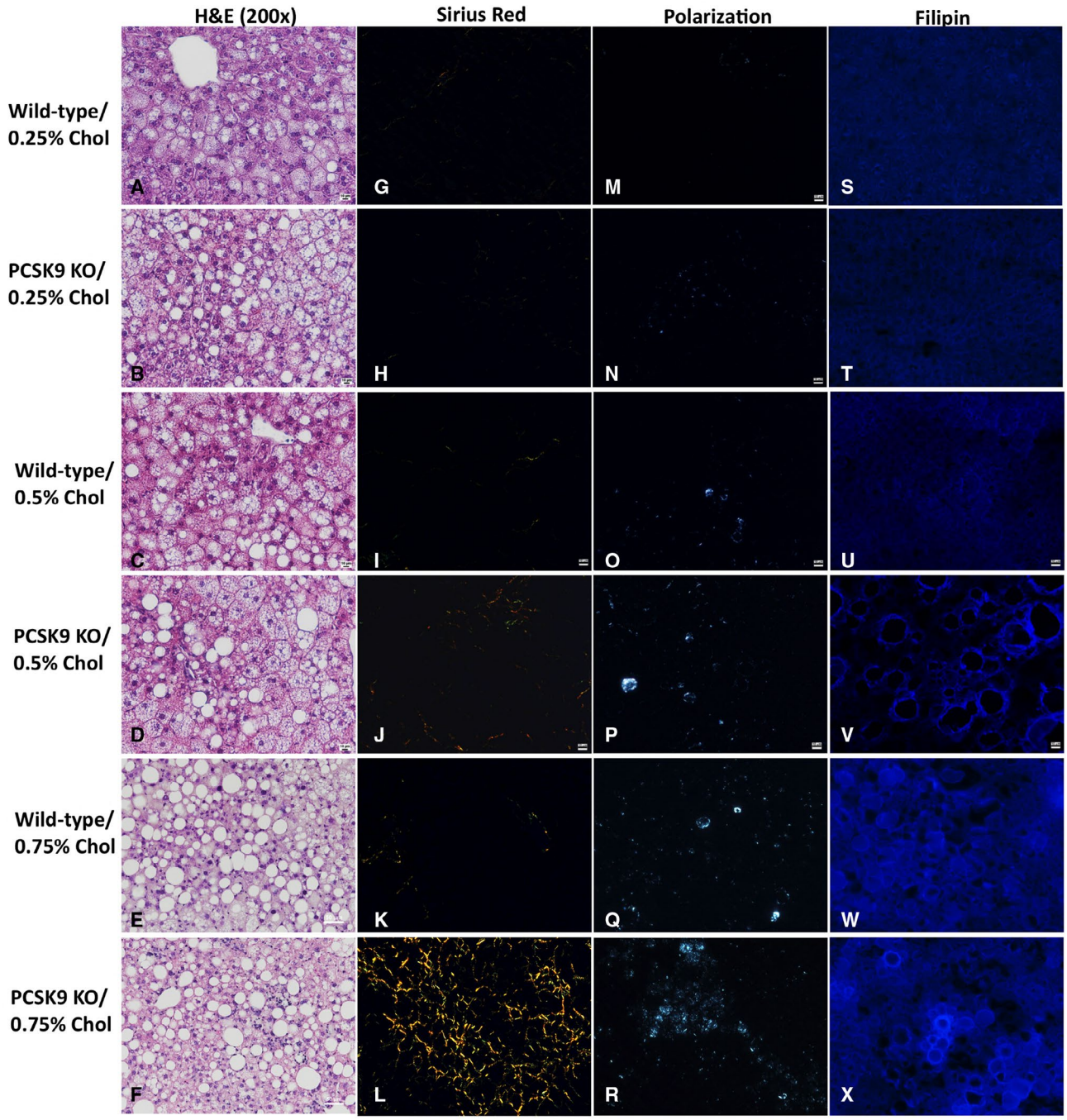

FIG. 1. Liver sections comparing WT versus *Pcsk9* KO mice after 9 months on high-fat (15%) diets supplemented with different concentrations of dietary cholesterol (0.25%, 0.5%, and 0.75%). Sections (×200 magnification) were stained with hematoxylin and eosin (H&E) for general histology and necroinflammation, sirius red for fibrosis, and fillip for free cholesterol; unstained sections were viewed under polarized light to visualize birefringent cholesterol crystals. The number of mice in each group and statistical comparisons between groups are provided in Table 1.

higher serum ALT and AST levels and higher hepatic histological inflammation score (Table 1). Also, at the 0.5% and 0.75% cholesterol diets, the *Pcsk9* KO mice had a 5-fold and 11-fold, respectively, higher hepatic sirius red staining for fibrosis than the WT mice (Table 1 and Fig. 1). In contrast,

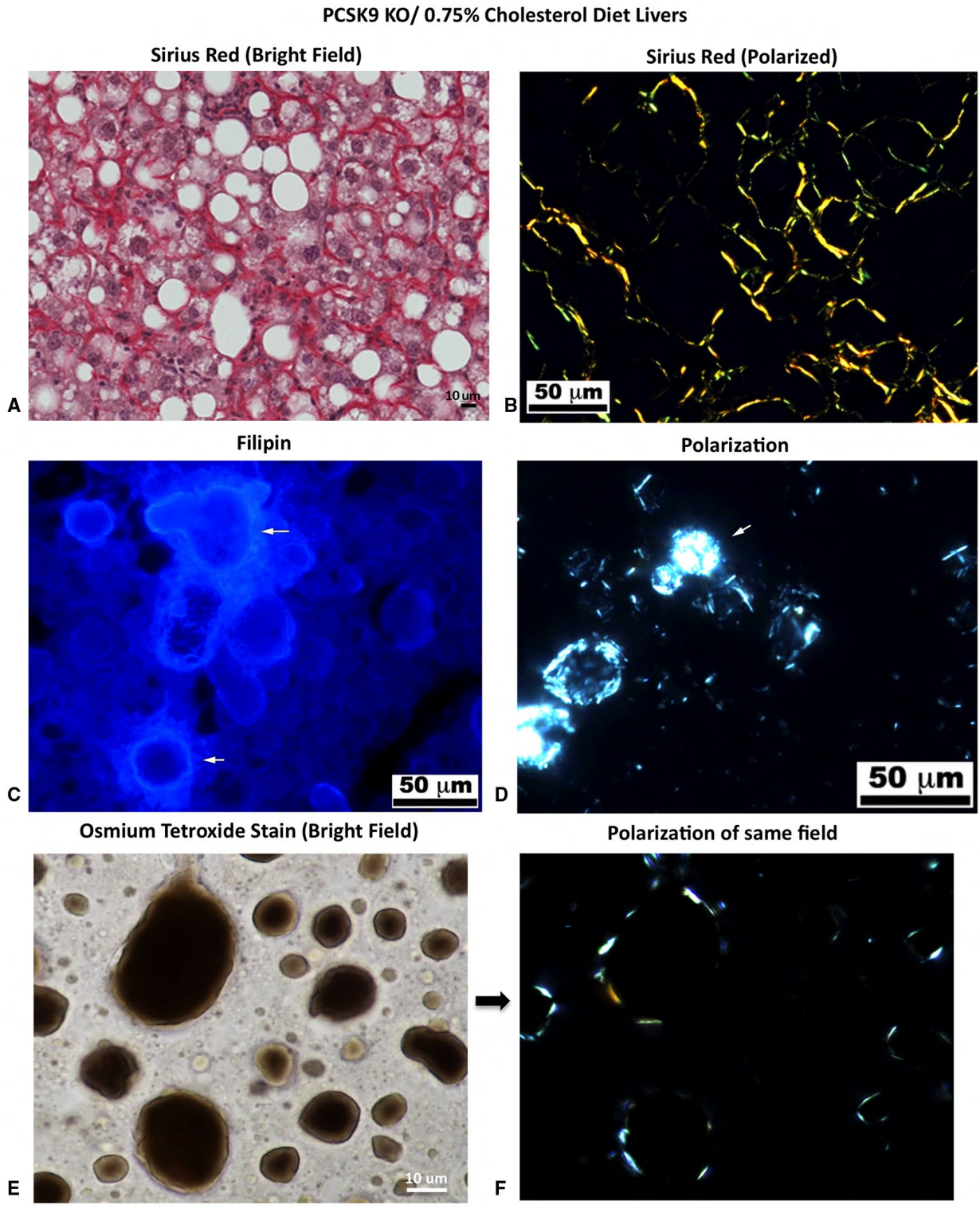

FIG. 2. Liver sections of *Pcsk9* KO mice on a high-fat (15%) and high-cholesterol (0.75%) diet for 9 months. Liver sections in *Pcsk9* KO mice demonstrate profound perisinusoidal fibrosis, evident with sirius red staining (A,B), and free cholesterol accumulation in lipid droplets by filipin stain (C), which also exhibits birefringence under polarized light (D) suggestive of crystallization. Staining with osmium tetroxide highlights the lipid droplets (E) and demonstrates cholesterol crystals in the periphery of these lipid droplets under polarized light (F).

TABLE 2. COMPARISON OF HEPATIC LIPID ANALYSIS AND HISTOCHEMISTRY ANALYSIS FOR LDLR, MACROPHAGE, AND APOPTOSIS IN WT VERSUS *PCSK9* KO MICE FED A HIGH-FAT, HIGH-CHOLESTEROL (0.75%) DIET

Genetic Background	WT (n = 12)	*Pcsk9* KO (n = 12)
Diet	0.75% Cholesterol	0.75% Cholesterol
HEPATIC LIPID COMPOSITION‡ (% of total lipid)		
Triglyceride	65.1 ± 9.3	63.2 ± 6.6
Cholesterol ester	15.7 ± 8.14	19.8 ± 4.0
Free cholesterol	1.53 ± 0.93	2.90 ± 0.93*
Free fatty acids	3.7 ± 1.3	4.3 ± 1.5
Phosphatidylcholine	7.7 ± 2.7	6.6 ± 1.0
Phosphatidylethanolamine	2.9 ± 1.2	2.4 ± 0.45
HEPATIC LIPID CONCENTRATION‡ (mg/g liver)		
Triglyceride	401.8 ± 137.4	243.6 ± 137.4*
Cholesterol esters	22.17 ± 12.15	17.53 ± 7.99
Free cholesterol	1.38 ± 0.31	1.67 ± 0.27*
Free fatty acids	2.16 ± 0.46	1.56 ± 0.48*
Phosphatidylcholine	12.59 ± 1.74	6.96 ± 2.63*
Phosphatidylethanolamine	5.07 ± 1.13	2.47 ± 0.96*
BILE ACID CONCENTRATION (μg/g liver)		
Total bile acids	86.1 ± 26.6	98.0 ± 8.2
Primary bile acids	71.2 ± 24.1	84.4 ± 7.2
Secondary bile acids	14.9 ± 5.2	13.6 ± 3.1
Unconjugated bile acids	17.6 ± 10.0	12.8 ± 3.0
Conjugated bile acids	68.5 ± 20.9	85.3 ± 8.4
HISTOCHEMICAL ANALYSIS		
LDLR, mean pixel intensity/×200 field§	1466.0 ± 201.3	1804.8 ± 207.6†
CD68 staining (macrophages), % area	0.66 ± 0.27	1.58 ± 0.69†
TUNEL (apoptosis), # TUNEL positive cells/×100 field	6.1 ± 4.4	15.9 ± 6.1†

*P value < 0.05.
†P value < 0.01.
‡"Composition" expresses each lipid as a percentage of all lipids by weight, and "concentration" presents the quantity of each lipid per gram of liver.
§LDLR immunohistochemistry was performed to confirm higher expression in the *Pcsk9* KO mice as expected and as described previously.

at the lower cholesterol diet (0.25%), hepatic necroinflammation (grade 1) and fibrosis (stage 0) were very low, with no significant differences between *Pcsk9* KO and WT mice.

Pcsk9 KO mice on 0.75% cholesterol diet had a 2.6-times increase in TUNEL-positive cells (apoptosis) and a 2.4-times increase in anti-CD68 staining for macrophages (Table 2 and Fig. 3). Anti-CD68-positive macrophages clustered around cholesterol crystal containing hepatocytes and lipid droplets forming crown-like structures (Fig. 3), as previously described,[14-17] in *Pcsk9* KO but not WT mice.

Pcsk9 KO mice had higher serum glucose and insulin levels at each dietary cholesterol level, resulting in significantly higher calculated level of Homeostasis Model Assessment–Insulin Resistance (HOMA-IR). However, *Pcsk9* KO mice had higher levels of HMW adiponectin and, as expected, lower plasma cholesterol levels.

PCSK9 KO MICE HAVE HIGHER HEPATIC EXPRESSION OF FIBROSIS AND INFLAMMATION-RELATED GENES THAN WT MICE WITH NO SIGNIFICANT DIFFERENCES IN CHOLESTEROL-RELATED GENES

Pcsk9 KO mice had significantly higher expression of hepatic fibrosis–related genes compared with WT mice (Table 3). Also, most hepatic inflammation-related genes had higher expression in *Pcsk9* KO mice, although this did not reach statistical

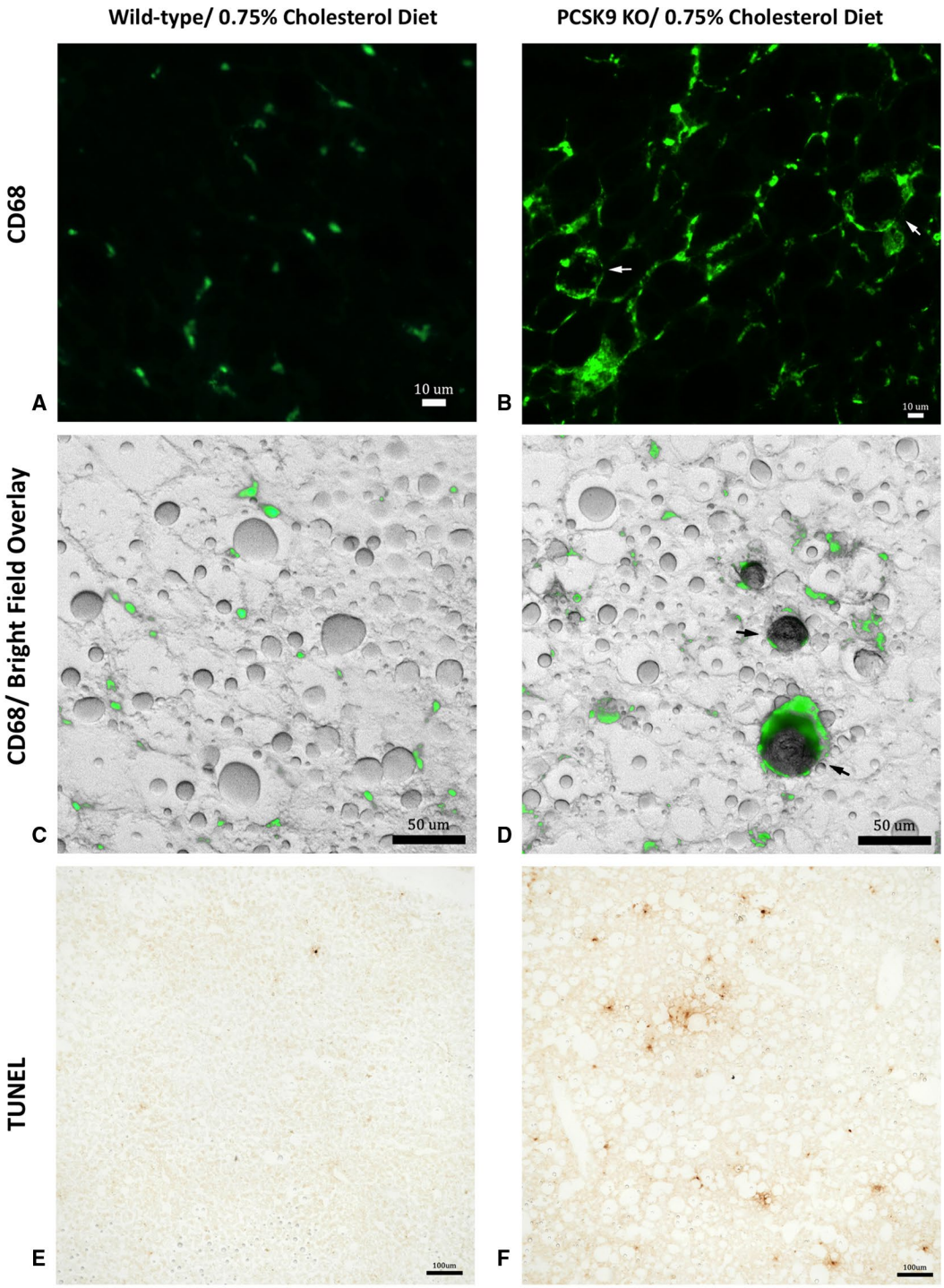

FIG. 3. Liver sections of *Pcsk9* KO versus WT mice on a high-fat (15%), high-cholesterol (0.75%) diet for 9 months. Anti-CD68 staining for macrophages (Kupffer cells) shows dramatically increased staining (green) in Pcsk9 KO (A) versus WT (B) mice, as well as patterns of macrophages forming circular crown-like structures in the *Pcsk9* KO mice. (D) The crown-like structures (arrows) of macrophages (green) are clustered around large lipid droplets with crystallized cholesterol (dark gray) in *Pcsk9* KO mice. TUNEL-positive apoptotic cells were much more common in liver sections from *Pcsk9* KO mice (F) than WT mice (E).

TABLE 3. COMPARISON OF *PCSK9* KO (N = 12) VERSUS WT MICE (N = 12) ON 0.75% CHOLESTEROL DIET WITH RESPECT TO HEPATIC GENE EXPRESSION (MRNA) OF SELECTED CRITICAL GENES RELATED TO HEPATIC FIBROSIS, INFLAMMATION, AND CHOLESTEROL HOMEOSTASIS

Name of Gene	LogFC*	Adjusted *P* Value†
FIBROSIS		
Collagen, type I, alpha 2 (*Col1a2*)	1.77	0.0518
Collagen, type III, alpha 1 (*Col3a1*)	1.67	0.0220
Collagen, type IV, alpha 1 (*Col4a1*)	1.24	0.0549
Collagen, type IV, alpha 2 (*Col4a2*)	1.58	0.0390
Collagen, type V, alpha 2 (*Col5a2*)	2.60	0.0407
Collagen, type VI, alpha 2 (*Col6a2*)	1.66	0.0384
Collagen, type VI, alpha 3 (*Col6a3*)	2.56	0.0253
Laminin, beta 2 (*Lamb2*)	1.72	0.0134
Tissue inhibitor of metalloproteinase 2 (*Timp2*)	1.18	0.0400
Matrix metallopeptidase 2 (*Mmp2*)	1.77	0.0119
Matrix metallopeptidase 14 (*Mmp14*)	0.81	0.0143
Smooth muscle actin (*Acta2*)	0.9185	0.3123
INFLAMMATION		
Tumor necrosis factor (*Tnf*)	1.48711	0.38445
Interleukin 1b (*Il1b*)	0.76571	0.63675
NLRP3 Inflammasome Protein (*Nlrp3*)	1.31065	0.41702
Caspase 1 (*CaspP1*)	1.30502	0.19999
Apoptosis-associated speck-like, caspase recruitment domain (CARD)–domain containing protein (*Asc/Pycard*)	1.34131	0.18809
Monocyte chemoattractant protein-1 (chemotactic factor) (*Ccl2*)	0.63265	0.58714
Serum amyloid A1 (pro-inflammatory factor) (*Saa1*)	0.08591	0.94404
EGF-like module-containing, mucin-like, hormone receptor-like 1 (*Emr1*)	1.27291	0.29696
Interleukin 7 receptor (*Il7r*)	2.95	0.0390
Caspase 4, apoptosis-related cysteine peptidase (*Casp4*)	3.14	0.0186
Transforming growth factor beta 1 induced transcript 1 (*Tgfb1i1*)	2.22	0.0551
Mediterranean fever (*Mefv*)	3.23	0.0407
CHOLESTEROL HOMEOSTASIS		
CHOLESTEROL SYNTHESIS		
3-hydroxy-3-methylglutaryl-coenzyme A reductase (*Hmgcr*)	–0.55087	0.68385
3-hydroxy-3-methylglutaryl-Coenzyme A synthase 1 (*Hmgcs1*)	–0.09977	0.92918
CHOLESTEROL EXPORT		
Abcg5	–0.06835	0.87862
Abcg8	–0.28852	0.40053
CHOLESTEROL UPTAKE		
Scavenger receptor SR-B1 = Cd36 (*Scarb1*)	–0.12394	0.67007
Low-density lipoprotein receptor (*Ldlr*)	–0.28603	0.48506
Proprotein convertase subtilisin/kexin type 9 (*Pcsk9*)	–4.58428	**0.01566**
BILE ACID SYNTHESIS		
Cytochrome P450 7A1 (*Cyp7a1*)	0.10658	0.92439
Cytochrome P450 27A1 (*Cyp27a1*)	–0.19139	0.25855
VLDL SYNTHESIS		
Microsomal triglyceride transfer protein (*Mttp*)	–0.13755	0.53292
CHOLESTEROL ESTERIFICATION		
Acetyl-coenzyme A acetyltransferase 2 (*Acat2*)	–0.46627	0.35952
TRANSCRIPTION FACTORS RELATED TO CHOLESTEROL AND BILE ACIDS		
LXR: nuclear receptor subfamily 1, group H, member 3	–0.02822	0.91985
FXR: nuclear receptor subfamily 1, group H, member 4	–0.18584	0.47861
Peroxisome proliferator activated receptor alpha (*Ppara*)	–0.12476	0.70663

TABLE 3. *Continued*

Name of Gene	LogFC*	Adjusted *P* Value†
Sterol regulatory element binding transcription factor 1 (Srebf1)	0.01734	0.98039
Sterol regulatory element binding transcription factor 2 (Srebf2)	0.03177	0.97165
FATTY ACID OXIDTION OR ESTERIFICATION		
Fatty acid synthase (*Fasn*)	–0.10316	0.93755
Stearoyl-coenzyme A desaturase 1 (*Scd1*)	–0.10315	0.57406
LIPID DROPLET PROTEINS		
Perilipin 1 (*Plin1*)	ND	ND
Perilipin 2 = ADFP = adipolipin (*Plin2*)	–0.07629	0.65582

*__LogFC is the Log2(fold change)__. Positive logFC number denotes that the gene has greater expression in the PCSK9 KO liver compared to WT liver, while a negative logFC number denotes that the gene has lower expression in the PCSK9 KO liver compared to WT Liver.
†Adjusted *P* value ≤ 0.05 when considered statistically different. Adjusted *P* value = false discovery rate.
Abbreviation: ND, not detected (no measurable expression of Plin1 in either group.

significance for most of these genes. In contrast, the genes related to critical cholesterol homeostasis pathways in the liver were not significantly differentially expressed in *Pcsk9* KO versus WT mice. Complete RNA-sequencing results are attached as Supporting Information.

PCSK9 KO MICE INJECTED WITH DEN DEVELOPED LIVER CANCER BUT NOT WT MICE

Three of six DEN-injected *Pcsk9* KO mice developed liver cancers that were macroscopically visible at the time of sacrifice and liver harvest and confirmed by sectioning and histological evaluation (Fig. 4). None of the six DEN-injected WT mice had liver cancer in their harvested livers after sectioning and histological examination of all liver segments.

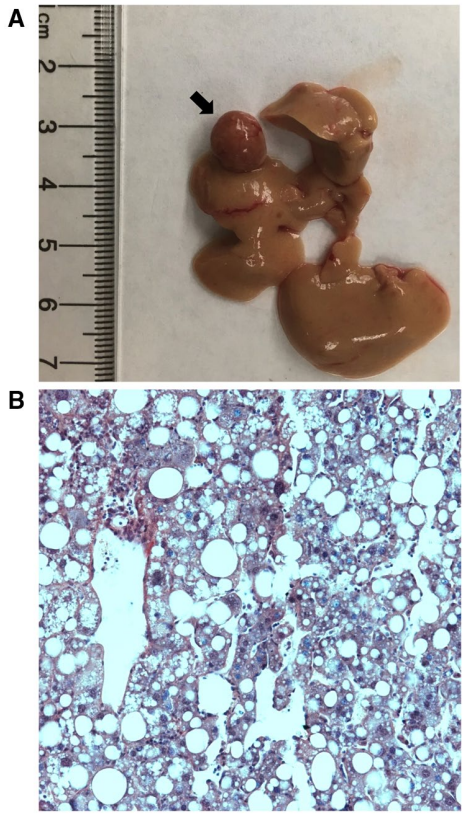

FIG. 4. (A) Exophytic liver cancer (arrow) identified at the time of sacrifice in a *Pcsk9* KO mouse that was injected with DEN at 5 weeks of age and then maintained on a 0.75% cholesterol diet for 9 months before sacrifice. (B) Representative sections of this liver cancer demonstrating lack of portal tracts and thickened trabecula, features of hepatocellular carcinoma.

Discussion

Pcsk9 KO mice on a high-fat, high-cholesterol diet exhibit higher levels of hepatic free cholesterol loading and hepatic cholesterol crystallization than their WT counterparts and develop significantly more hepatic inflammation and fibrosis associated with the development of macrophage crown-like structures. When injected with DEN early in life, *Pcsk9* KO mice were likely to develop liver cancer, but not WT mice. Our results suggest that genetic deletion of the *Pcsk9* gene results in higher cholesterol uptake by the liver via LDLR and hepatic cholesterol loading, predisposing to fibrosing steatohepatitis and hepatic carcinogenesis. These findings may have implications for the long-term use of PCSK9 inhibitors (alirocumab, evolocumab) in the treatment of hypercholesterolemia in humans.

Our results are consistent with a prior study by Lebeau et al.,[25] but extend our understanding of the impact of *Pcsk9* deletion on murine NASH in important ways. In Lebeau et al., *Pcsk9* KO mice exposed to a high-fat diet (without excess dietary cholesterol) for 12 weeks appeared to have more hepatic steatosis and higher ALT than WT mice.[25] However, a very small number of mice were used (n = 5 per group) and the mice did not develop substantial fibrosis (likely due to young age, short duration, and absence of excess dietary cholesterol). Fibrosis is the most important determinant of long-term outcomes in NASH. We specifically wanted to study the role of *Pcsk9* deletion in the setting of exposure to high-cholesterol diet in a mouse model that develops profound *fibrosing* steatohepatitis. Our most important result is that *Pcsk9* KO mice had a 5-fold (at 0.5% dietary cholesterol) and 11-fold (at 0.75% dietary cholesterol) higher hepatic fibrosis (assessed by sirius red staining) than WT mice, whereas hepatic free cholesterol was the only lipid that was significantly higher in the *Pcsk9* KO mice; in fact, hepatic triglyceride concentration was significantly lower (possibly related to the profound necroinflammation and fibrosis in the *Pcsk9* KO mice), thus completely dissociating the impact of free cholesterol from that of triglycerides.[26] Also, our finding that following DEN injection, three of six *Pcsk9* KO mice developed liver cancer versus none of the six WT mice is very intriguing, given recent advances in the understanding of the role of cholesterol in hepatocarcinogenesis.[27] Unfortunately, additional DEN injections experiments that we initiated had to be terminated due to animal distress; hence, our results on hepatocarcinogenesis need to be confirmed by future studies.

Excess hepatic cholesterol has been shown to promote NASH in a variety of animal models,[14,16,21,28,29] through mechanisms involving endoplasmic reticulum (ER) stress, mitochondrial dysfunction, development of toxic oxysterols, or stabilization of the transcription factor TAZ.[30] We also demonstrated that in murine models of NASH driven by high-fat, high-cholesterol diets, excess cholesterol crystallizes in hepatocyte lipid droplets, and these cholesterol crystals might promote necroinflammation in NASH.[14-17] Here we also demonstrate increased hepatic free cholesterol and cholesterol crystallization in the *Pcsk9* KO mice on 0.75% dietary cholesterol together with formation of "crown-like structures" of CD68-positive macrophages that surround and process hepatocytes and lipid droplets with cholesterol crystals (Fig. 2), which may initiate and propagate the "sterile inflammation" of NASH.

Fold-change overload in hepatocytes can lead to ER stress, mitochondrial dysfunction, development of toxic oxysterols, and cholesterol crystallization in lipid droplets, which, in turn, lead to hepatocyte apoptosis, necrosis, or pyroptosis. Activation of Kupffer cells and hepatic stellate cells by hepatocyte signaling and cholesterol loading contributes to this inflammation and leads to hepatic fibrosis.

Studies of the impact of loss-of-function mutations in the *PCSK9* gene on NAFLD in humans might be expected to shed light on the role of Pcsk9 inhibition in NASH; however, they have yielded mixed results. In some studies, loss-of-function *PCSK9* mutations have been associated with hepatic steatosis as well as very low levels of circulating LDL-C.[2,3] Hepatic steatosis was present in 64.3% of carriers of the R46L variant of the *PCSK9* gene, which is a loss-of-function mutation, compared to 35.2% of noncarriers, and severe steatosis was present in 7.2% of carriers versus 2.0% of noncarriers, together with a significant increase in serum AST.[31] These findings would appear to support our hypothesis that inhibition of PCSK9 might result in excess hepatic steatosis and steatohepatitis. However, in other studies the loss-of-function R46L *PCSK9* variant was not associated with increased liver enzymes or with suspected NAFLD, identified by a natural language processing algorithm.[32] None of these studies investigated the impact of PCSK9 variants on NASH rather than simply fatty liver. Furthermore, these results are confounded by the potential effects to the liver of the defective protein itself that fails to undergo appropriate processing in the ER.[33]

Some human studies demonstrated an association between increased plasma PCSK9 levels and increased hepatic steatosis and liver enzymes.[34,35] This may appear contradictory to our findings, as it would suggest that inhibiting PCSK9 might reduce hepatic steatosis and liver enzymes. However, such cross-sectional studies cannot distinguish cause from effect. For example, it is possible (in fact, more likely) that hepatic steatosis itself or factors associated with hepatic steatosis (e.g., metabolic syndrome, hyperlipidemia) resulted in an increase in plasma PCSK9 levels, rather than the other way round.[34] In support

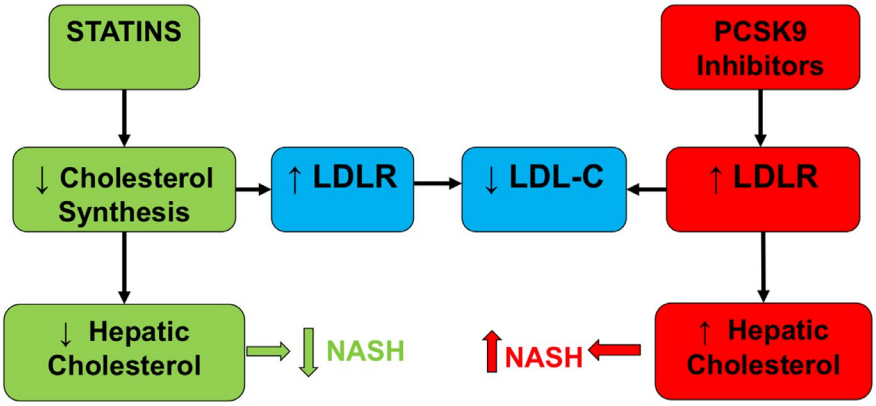

FIG. 5. Differences in the mechanisms of action of PCSK9 inhibitors versus statins may have differential effects on hepatic cholesterol levels and NASH. Both statins and PCSK9 inhibitors decrease plasma LDL-cholesterol. However, statins inhibit hepatic cholesterol synthesis and thereby decrease hepatic cholesterol, which may have beneficial effects on NASH. In contrast, PCSK9 inhibitors increase the expression of LDLR by the liver, resulting in greater uptake of LDL-cholesterol, and increase hepatic cholesterol, which may have detrimental effects on NASH.

of this hypothesis, diet-induced hepatic steatosis was shown to induce *de novo* PCSK9 expression in mice and reduce LDLR expression.[36]

A systematic review and meta-analysis of randomized controlled trials of alirocumab or evolocumab did not find evidence of increased risk of acute liver enzyme elevations (>3 times the upper limit of normal) compared with placebo.[5] Although this excludes an increased risk of acute liver injury related to PCSK9 inhibitors, it does not exclude chronic liver injury, such as that related to increased hepatic cholesterol levels, which would manifest with very mild liver enzyme elevations. Furthermore, in these human studies, all patients who were randomized to PCSK9 inhibitors versus placebo were on a statin, which could have protected the liver from excess cholesterol, thereby masking any potential negative effects of PCSK9 inhibitors.

Both statins and PCSK9 inhibitors reduce plasma LDL-C levels. However, their mechanism of action is fundamentally different, such that statins result in lowering of hepatic cholesterol levels whereas PCSK9 inhibition may result in increased hepatic cholesterol levels (Fig. 5), as suggested by our findings, which may have dramatically different implications for the liver. Several lines of evidence suggest that hepatic cholesterol is an important etiologic factor that can lead to the development and progression from simple steatosis to fibrosing steatohepatitis, both in animal models and in humans.[13] In humans, hepatic free cholesterol levels were found to be elevated in NASH,[37] dietary cholesterol intake was associated with development of cirrhosis,[38] and statin use was associated with amelioration of hepatic steatosis, inflammation, and fibrosis.[6-11]

Metabolically, the *Pcsk9* KO mice exhibited a mixed profile. On the one hand, they appeared to have worse insulin resistance as estimated by HOMA-IR, possibly related to the excess hepatic cholesterol levels and necroinflammation. However, they had significantly higher HMW adiponectin levels, likely related to lower levels of circulating lipoproteins and reduced adipose tissue inflammation.

Pcsk9 is expressed predominantly in the liver, but also demonstates lower expression in intestine. Because we used global Pcsk9 KO mice, we cannot distinguish effects mediated though hepatic expression versus expression in other tissues. Our experimental design does not allow us to prove whether the more advanced NASH that was observed in the *Pcsk9* KO mice was directly caused by higher hepatic free cholesterol levels. However, we used a mouse model in which the fibrosing steatohepatitis is known to be directly linked to dietary cholesterol and the accumulation of hepatic cholesterol and cholesterol crystals.[15] Although *Pcsk9* KO mice had the same mixed B6;129 background as the WT mice, they were not littermates; hence, they may have

had minor strain differences. In addition to LDLR, secreted PCSK9 has recently been shown to promote the degradation of other receptors involved in the uptake of circulating lipids by the liver (e.g., very low density lipoprotein receptor, LDLR-related protein-1, ApoE receptor-2, and CD36). Our experimental design does not allow us to distinguish these mechanisms of action, but all would result in less hepatic lipid uptake following *Pcsk9* deletion. In addition, future experiments that use pharmacologic inhibition of Pcsk9 (rather than genetic deletion) may be more directly relevant to the effects of Pcsk9 inhibitors.

In conclusion, *Pcsk9* KO mice on high-cholesterol diets develop increased hepatic free cholesterol and cholesterol crystals and fibrosing steatohepatitis with a higher predisposition to liver cancer. Studies should evaluate whether patients on long-term treatment with anti-PSCK9 monoclonal antibodies are at increased risk of hepatic steatosis, steatohepatitis or liver cancer, while accounting for concurrent use of statins.

REFERENCES

1) Rashid S, Curtis DE, Garuti R, Anderson NN, Bashmakov Y, Ho YK, et al. Decreased plasma cholesterol and hypersensitivity to statins in mice lacking Pcsk9. Proc Natl Acad Sci U S A 2005;102:5374-5379.
2) Fasano T, Cefalu AB, Di Leo E, Noto D, Pollaccia D, Bocchi L, et al. A novel loss of function mutation of PCSK9 gene in white subjects with low-plasma low-density lipoprotein cholesterol. Arterioscler Thromb Vasc Biol 2007;27:677-681.
3) Cariou B, Ouguerram K, Zaïr Y, Guerois R, Langhi Cédric, Kourimate S, et al. PCSK9 dominant negative mutant results in increased LDL catabolic rate and familial hypobetalipoproteinemia. Arterioscler Thromb Vasc Biol 2009;29:2191-2197.
4) Horton JD, Cohen JC, Hobbs HH. Molecular biology of PCSK9: its role in LDL metabolism. Trends Biochem Sci 2007;32:71-77.
5) Guedeney P, Giustino G, Sorrentino S, Claessen BE, Camaj A, Kalkman DN, et al. Efficacy and safety of alirocumab and evolocumab: a systematic review and meta-analysis of randomized controlled trials. Eur Heart J 2019 Jul 3. https://doi.org/10.1093/eurheartj/ehz430. [Epub ahead of print]
6) Athyros VG, Tziomalos K, Gossios TD, Griva T, Anagnostis P, Kargiotis K, et al. Safety and efficacy of long-term statin treatment for cardiovascular events in patients with coronary heart disease and abnormal liver tests in the Greek Atorvastatin and Coronary Heart Disease Evaluation (GREACE) study: a post-hoc analysis. Lancet 2010;376:1916-1922.
7) Athyros VG, Mikhailidis DP, Didangelos TP, Giouleme OI, Liberopoulos EN, Karagiannis A, et al. Effect of multifactorial treatment on non-alcoholic fatty liver disease in metabolic syndrome: a randomised study. Curr Med Res Opin 2006;22:873-883.
8) Foster T, Budoff MJ, Saab S, Ahmadi N, Gordon C, Guerci AD. Atorvastatin and antioxidants for the treatment of nonalcoholic fatty liver disease: the St Francis Heart Study randomized clinical trial. Am J Gastroenterol 2011;106:71-77.
9) Nelson A, Torres DM, Morgan AE, Fincke C, Harrison SA. A pilot study using simvastatin in the treatment of nonalcoholic steatohepatitis: a randomized placebo-controlled trial. J Clin Gastroenterol 2009;43:990-994.
10) Dongiovanni P, Petta S, Mannisto V, Mancina RM, Pipitone R, Karja V, et al. Statin use and non-alcoholic steatohepatitis in at risk individuals. J Hepatol 2015;63:705-712.
11) Kargiotis K, Athyros VG, Giouleme O, Katsiki N, Katsiki E, Anagnostis P, et al. Resolution of non-alcoholic steatohepatitis by rosuvastatin monotherapy in patients with metabolic syndrome. World J Gastroenterol 2015;21:7860-7868.
12) Theocharidou E, Papademetriou M, Reklou A, Sachinidis A, Boutari C, Giouleme O. The role of PCSK9 in the pathogenesis of non-alcoholic fatty liver disease and the effect of PCSK9 inhibitors. Curr Pharm Des 2018;24:3654-3657.
13) Ioannou GN. The role of cholesterol in the pathogenesis of NASH. Trends Endocrinol Metab 2016;27:84-95.
14) Ioannou GN, Haigh WG, Thorning D, Savard C. Hepatic cholesterol crystals and crown-like structures distinguish NASH from simple steatosis. J Lipid Res 2013;54:1326-1334.
15) Ioannou GN, Subramanian S, Chait A, Haigh WG, Yeh MM, Farrell GC, et al. Cholesterol crystallization within hepatocyte lipid droplets and its role in murine NASH. J Lipid Res 2017;58:1067-1079.
16) Ioannou GN, Van Rooyen DM, Savard C, Haigh WG, Yeh MM, Teoh NC, et al. Cholesterol-lowering drugs cause dissolution of cholesterol crystals and disperse Kupffer cell crown-like structures during resolution of NASH. J Lipid Res 2015;56:277-285.
17) Ioannou GN, Landis CS, Jin G-Y, Haigh WG, Farrell GC, Kuver R, et al. Cholesterol crystals in hepatocyte lipid droplets are strongly associated with human nonalcoholic steatohepatitis. Hepatol Commun 2019;3:776-791.
18) Tolba R, Kraus T, Liedtke C, Schwarz M, Weiskirchen R. Diethylnitrosamine (DEN)-induced carcinogenic liver injury in mice. Lab Anim 2015;49:59-69.
19) Bakiri L, Hamacher R, Grana O, Guio-Carrion A, Campos-Olivas R, Martinez L, et al. Liver carcinogenesis by FOS-dependent inflammation and cholesterol dysregulation. J Exp Med 2017;214:1387-1409.
20) Kleiner DE, Brunt EM, Van Natta M, Behling C, Contos MJ, Cummings OW, et al. Design and validation of a histological scoring system for nonalcoholic fatty liver disease. Hepatology 2005;41:1313-1321.
21) Savard C, Tartaglione EV, Kuver R, Haigh WG, Farrell GC, Subramanian S, et al. Synergistic interaction of dietary cholesterol and dietary fat in inducing experimental steatohepatitis. Hepatology 2013;57:81-92.
22) Rudolf M, Curcio CA. Esterified cholesterol is highly localized to Bruch's membrane, as revealed by lipid histochemistry in wholemounts of human choroid. J Histochem Cytochem 2009;57:731-739.
23) Gomez MV, Dutta M, Suvorov A, Shi X, Gu H, Mani S, et al. Early life exposure to environmental contaminants (BDE-47, TBBPA, and BPS) produced persistent alterations in fecal microbiome in adult male mice. Toxicol Sci 2021;179:14-30.
24) Finak G, McDavid A, Yajima M, Deng J, Gersuk V, Shalek AK, et al. MAST: a flexible statistical framework for assessing transcriptional changes and characterizing heterogeneity in single-cell RNA sequencing data. Genome Biol 2015;16:278.
25) Lebeau PF, Byun JH, Platko K, Al-Hashimi AA, Lhoták Š, MacDonald ME, et al. Pcsk9 knockout exacerbates diet-induced non-alcoholic steatohepatitis, fibrosis and liver injury in mice. JHEP Rep 2019;1:418-429.

26) Yamaguchi K, Yang L, McCall S, Huang J, Yu XX, Pandey SK, et al. Inhibiting triglyceride synthesis improves hepatic steatosis but exacerbates liver damage and fibrosis in obese mice with nonalcoholic steatohepatitis. Hepatology 2007;45:1366-1374.
27) Liang JQ, Teoh N, Xu L, Pok S, Li X, Chu ESH, et al. Dietary cholesterol promotes steatohepatitis related hepatocellular carcinoma through dysregulated metabolism and calcium signaling. Nat Commun 2018;9:4490.
28) Subramanian S, Goodspeed L, Wang S, Kim J, Zeng L, Ioannou GN, et al. Dietary cholesterol exacerbates hepatic steatosis and inflammation in obese LDL receptor-deficient mice. J Lipid Res 2011;52:1626-1635.
29) Van Rooyen DM, Larter CZ, Haigh WG, Yeh MM, Ioannou G, Kuver R, et al. Hepatic free cholesterol accumulates in obese, diabetic mice and causes nonalcoholic steatohepatitis. Gastroenterology 2011;141:1393-4403, 1403.e1–5.
30) Horn CL, Morales AL, Savard C, Farrell GC, Ioannou GN. Role of cholesterol-associated steatohepatitis in the development of NASH. Hepatol Commun 2021. https://doi.org/10.1002/hep4.1801. [Epub ahead of print]
31) Baragetti A, Balzarotti G, Grigore L, Pellegatta F, Guerrini U, Pisano G, et al. PCSK9 deficiency results in increased ectopic fat accumulation in experimental models and in humans. Eur J Prev Cardiol 2017;24:1870-1877.
32) Rimbert A, Smati S, Dijk W, Le May C, Cariou B. Genetic Inhibition of PCSK9 and liver function. JAMA Cardiol 2021;6:353-354.
33) Lebeau PF, Wassef H, Byun JH, Platko K, Ason B, Jackson S, et al. The loss-of-function PCSK9Q152H variant increases ER chaperones GRP78 and GRP94 and protects against liver injury. J Clin Invest 2021;131:e128650.
34) Ruscica M, Ferri N, Macchi C, Meroni M, Lanti C, Ricci C, et al. Liver fat accumulation is associated with circulating PCSK9. Ann Med 2016;48:384-391.
35) Paquette M, Gauthier D, Chamberland A, Prat A, De Lucia Rolfe E, Rasmussen JJ, et al. Circulating PCSK9 is associated with liver biomarkers and hepatic steatosis. Clin Biochem 2020;77:20-25.
36) Lebeau PF, Byun JH, Platko K, MacDonald ME, Poon SV, Faiyaz M, et al. Diet-induced hepatic steatosis abrogates cell-surface LDLR by inducing de novo PCSK9 expression in mice. J Biol Chem 2019;294:9037-9047.
37) Puri P, Baillie RA, Wiest MM, Mirshahi F, Choudhury J, Cheung O, et al. A lipidomic analysis of nonalcoholic fatty liver disease. Hepatology 2007;46:1081-1090.
38) Ioannou GN, Morrow OB, Connole ML, Lee SP. Association between dietary nutrient composition and the incidence of cirrhosis or liver cancer in the United States population. Hepatology 2009;50:175-184.

Supporting Information

Additional Supporting Information may be found at onlinelibrary.wiley.com/doi/10.1002/hep4.1858/suppinfo.